CHEMICAL ENGINEERING TRANSACTIONS

VOL. 70, 2018

A publication of
AIDIC
The Italian Association
of Chemical Engineering
Online at www.aidic.it/cet

Guest Editors: Timothy G. Walmsley, Petar S. Varbanov, Rongxin Su, Jiří J. Klemeš

ISBN 978-88-95608-67-9; **ISSN** 2283-9216

DOI: 10.3303/CET1870304

Synthesis of Core-Shell Nanoparticles for the Removal of Toxic Pollutants in Aqueous Medium

Srikanth Vuppala[a,*], Marco Stoller[b], Agostina Chiavola[c], Andrei Kanaev[d], Khley Cheng[d]

[a]Dept. Of Astronautics Electrical and Energy Engineering, University of Rome “La Sapienza”, Via Eudossiana, 18, 00184, Rome, Italy
[b]Department of Chemical Materials Environmental Engineering, ‘La Sapienza’ University of Rome, Via Eudossiana 18, 00184, Rome, Italy,
[c]Department of Civil, Building and Environmental Engineering, Faculty of Civil and Industrial Engineering, Sapienza University of Rome, Via Eudossiana 18, Zip code 00184, Rome, Italy,
[d]Laboratoire des Sciences des Procédés et des Matériaux, CNRS, Université Paris 13, Sorbonne Paris Cité, 93430, Villetaneuse, France
srikanth.vuppala@uniroma1.it

In this work two active photo-catalysts were synthetized and tested for the removal of methylene blue and arsenic in aqueous solutions. The two catalysts ($Fe_3O_4/SiO_2/TiO_2$-Al and Fe_3O_4-SiO_2/Zr-TiO_2) were characterized by nano-size, guaranteeing a large specific surface area and a noticeable number of active sites and resulted active in the visible spectra (400-800 nm). The nanoparticles were characterized by BET, FE-SEM and EDS methods. The two nano-materials showed high As and methylene blue removal efficiency and were tested varying the contact time from 1 h up to 24 h. The $Fe_3O_4/SiO_2/TiO_2$-Al nanoparticles demonstrated to be more versatile, since showed a noticeable removal efficiency considering both pollutants As (73.5 %) and methylene blue (78 %) after 24 h. The Fe_3O_4-SiO_2/Zr-TiO_2) nanoparticles showed a higher affinity towards methylene blue removal (90.5 %) whereas the As removal efficiency was negligible (0.5 %). The two nano-materials were tested also in a bi-component solution, loading both As and methylene blue target pollutants.

1. Introduction

The quality of water would be an area of concern in upcoming future due to wide spreading pollution (Bavasso et al., 2016). Presently, around 700 million individuals in 43 nations are victims to the effects of water shortage and by 2025, 1.8 billion individuals will live in nations or areas with supreme water shortage (Vilardi et al., 2017a). About 66 % of the total population could be living under water stressed conditions (Ruzmanova et al., 2015). Various researchers deeply investigated heterogeneous photocatalysis (Stoller et al., 2011), that was considered a possible solution to this problem (Stoller et al., 2016), because of its high potential to remove toxins and xenobiotics through entire mineralization in aqueous medium (Stoller et al., 2017a). Among the known semiconductor titanium dioxide, activated alumina are the most widely used due to its high catalytic activity, chemical stability and low cost (Chinh et al., 2018).

Magnetite nanoparticles have substantial specific surface area with a solid tunneling impact and a little size of the border effect (Vilardi et al., 2018a), which may be helpful for the adsorption procedure (Stoller et al., 2017b); besides, they have the general properties of conventional iron (Vilardi et al., 2018b) and in this way conceivably a high proclivity to arsenic and organic compounds (Di Palma et al., 2015). Magnetite is a normally occurring mineral (Vilardi et al., 2018c) but can be also easily prepared in the laboratory from solutions containing ferric and ferrous ions (Vilardi et al., 2018d). The iron nanoparticles have a uniform particle size (Muradova et al., 2016), high chemical activity (Vilardi, 2018), low presence of carbon, nitrogen, oxygen, sulfur, phosphorus and other active components (Vilardi et al., 2018e) and the capacity to remain in suspension for long time when injected as colloidal suspension into contaminated zone (Vilardi et al., 2017b).

Please cite this article as: Vuppala S., Stoller M., Chiavola A., Kanaev A., Cheng K., 2018, Synthesis of core-shell nanoparticles for the removal of toxic pollutants in aqueous medium , Chemical Engineering Transactions, 70, 1819-1824 DOI:10.3303/CET1870304

Past examinations have demonstrated the capacity of iron-based nanoparticles to remove various heavy metals, such as Cr(VI), both in soil (Gueye et al., 2016) and aqueous medium (Vilardi et al., 2017c) also in complex matrix (Vilardi et al., 2018f), U (Crespi et al., 2016), or inorganic ions, such as nitrates (Vilardi and Di Palma, 2017) and in particular, to decrease quickly arsenic concentration beneath the maximum level set for drinking water (Chiavola et al. 2017). Towards Cr(VI) and U the removal efficiency achieved with iron-based nanoparticles was significantly higher in comparison with that obtained by classical biological technologies (Marsili et al., 2005) using sulfate-reducing bacteria (Marsili et al., 2007).

Alumina has been widely investigated due to its potential capacity of adsorbing a wide range of contaminants, such as arsenic. Activated alumina (AA), prepared by thermal dehydration of aluminum hydroxide, has a high surface area and a distribution of both macro- and micro-pores, which make it more suitable for efficient uptake. The United Nations Environmental Program agency has classified AA adsorption among the best available technologies for arsenic removal from water.

Several studies have been performed to evaluate the adsorption capacity of TiO_2 for As (V) and As(III) removal from water (Chiavola et al. 2016). On the other hand, these materials are very costly (Vilardi et al., 2018b), and process feasibility can only be achieved if the adsorbent material may be regenerated and reused (Ruzmanova et al., 2013; Stoller et al., 2015). The ZrO_2-TiO_2 composite was observed to be a fascinating material for use as catalyst, supported catalyst and photo-catalyst: the mixed composite ZrO^2-TiO_2 photocatalyst has been used for the degradation of several organic compounds, such as trichloroethylene and methylene blue (Cheng et al., 2017).

In the present study, a three-stage synthesis method was adopted for preparation of core-shell-shell $Fe_3O_4/SiO_2/TiO_2$, $Fe_3O_4/SiO_2/Zr$-TiO_2, $Fe_3O_4/SiO_2/TiO_2$-Al, nanoparticles by means of Spinning Disk Reactor (SDR) (Rashid et al., 2015), as already done in previous studies (Vilardi et al., 2017b) and T-mixer (Cheng et al. 2017). The nanoparticles were evaluated on their efficiency to remove organic matter and metal: the first in terms of degradation of methylene blue in synthetic wastewater, and the second by arsenic adsorption capacity. At the end, the catalyst was recovered by application of an external magnetic field (magnets).

2. Materials and methods

2.1 Synthesis of Fe_3O_4-SiO_2 core-shell nanoparticles

The core-shell SiO_2/Fe_3O_4 nanoparticles (FM) were prepared by two steps. Firstly, Fe_3O_4 magnetic nanoparticles were synthesized using a spinning disk reactor. Then, FM nanoparticles were prepared by dispersing Fe_3O_4 particles in distilled water, followed by the addition of C_2H_5OH (Sigma Aldrich). Tetraethyl ortosilicate (TEOS), preliminarily diluted in C_2H_5OH, was added drop-wise to the Fe_3O_4 particle suspension. Then an aqueous solution of NH_3 (30 wt %) was added and the TEOS hydrolysis and condensation was allowed under overnight gentle stirring. The obtained FM particles were washed in a centrifuge using firstly water/ethanol mixtures then distilled water. Finally, they were dried and calcinated at 450 °C for 30 min (Vaiano et al., 2016).

2.2 Synthesis of Fe_3O_4-SiO_2/N-doped TiO_2 nanoparticles

Fe_3O_4-SiO_2/N-doped TiO_2 nanoparticles were prepared by adding urea in 50 mL of water under continuous stirring conditions for 10 min, then Fe/SiO_2 solution was sonicated for 5 min finally TTIP was added under sonication followed by 10 min mechanical mixing. The mixture was centrifuged and washed for two times. Finally, the recovered sample was calcinated at 450 °C for 30 min (Ramp 10°C/min) to obtain the final N-TiO_2/FM catalyst. The nominal loading of N-TiO_2 on the FM support was 37.5 %wt.

2.3 Synthesis of $Fe_3O_4/SiO_2/TiO_2$-Al nanoparticles (FMAL)

Fe_3O_4-SiO_2/N-doped TiO_2- Al nanoparticles were prepared by adding Alumina Isopropanol (solid) in 50 ml of isopropanol under continuous stirring conditions for 10 min, then FM/N-TiO_2 solution was sonicated for 5 min finally TTIP was added under sonication followed by 10 min mechanical mixing. The mixture was centrifuged and washed for two times. Finally, the recovered sample was calcinated at 450 °C/ 30 min (Ramp 10°C/min) to obtain the final N-TiO_2/FM-Al catalyst.

2.4 Synthesis of Fe_3O_4-SiO_2/Zr-TiO_2 nanoparticles (FMZR)

8.470 mL titanium(IV) isopropoxide (98 %), 0.654 mL zirconium(IV) propoxide (70 %) were added into n-propanol 40.876 mL and stirred 10 min. Then it was transferred into syringe in glove box to get solution A. 0.658 mL water is added into n-propanol 49.342 mL and stirred 10 min. Then it was transferred into syringe in glove box to get solution B, the solutions A and B were injected into the tanks of the reactor. The pressure nitrogen of 4 bar was applied to mix at T-mixer. The temperature 20 °C and humidity were controlled. The solution was transferred into the vial and brought into glove box. 11 g FM was coated by ZTOA in 10 min with stirring 1 min at the beginning. The coated FM by TOA nanoparticle was separated and then dried in oven at 80 °C for overnight. The dried materials were calcinated from 50 °C to 500 °C by rate 2 °C/min and kept 4 h.

2.5 Samples characterization

Physico-chemical samples characterization has been performed with different techniques. The specific surface area of the prepared nano-materials was measured by using a BET analyzer Nano Sord (NS). The average size and morphology of the nanoparticles was determined by SEM (FE-SEM HR Zeiss Auriga 405).

2.6 Experimental set-up

The experiments were carried out with initial concentration of Methylene Blue (MB) and As equal to 7 mg L^{-1} and 0.5 mg L^{-1}, respectively. The catalyst dosage was 3 g L^{-1}. The total volume of the solution was always 80mL. The experiments were conducted using a pyrex cylindrical photoreactor (ID=2.5 cm, height=25 cm) equipped with an air distributor device (Q_{air}=150 cm^3 min^{-1} (STP)). Continuous mixing of the aqueous solution was done by external recirculation of the same solution using a peristaltic pump. The photoreactor was irradiated with a strip composed of 25 Blue light LEDs (6W nominal power; provided by New Oralight, with wavelength emission in the range 400–800 nm with main emission peak at 475 nm. The LEDs strip was positioned around and in contact with the external surface of the photoreactor (incident light intensity 32 mW cm^{-2}). The residual concentration of MB in aqueous samples was monitored by observing the change in the absorbance at the maximum absorption wavelength of 668 nm using a UV–vis spectrophotometer (Lambda 35, Perkin Elmer), and then the concentration was calculated from a calibration curve. The As concentration was determined using a graphite tube atomizer (Agilent). The As adsorption tests were carried out without light irradiation.

3. Results and discussion

3.1 Sample characterization

The materials under testing during this work were analysed by SEM and EDS, as reported in Figure 1 and 2:

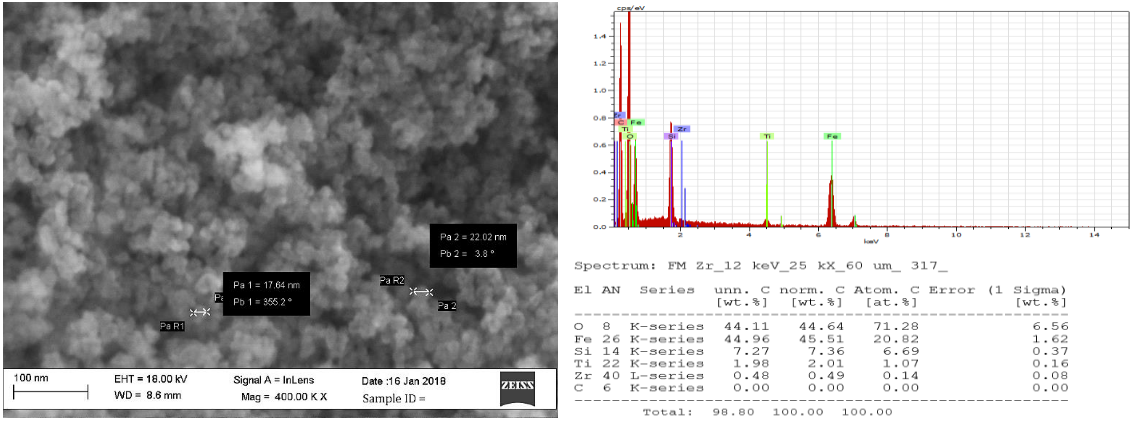

```
Spectrum: FM Zr_12 keV_25 kX_60 um_ 317_

El AN  Series   unn. C norm. C Atom. C Error (1 Sigma)
                [wt.%]  [wt.%]  [at.%]          [wt.%]
------------------------------------------------------
O   8  K-series  44.11   44.64   71.28            6.56
Fe 26  K-series  44.96   45.51   20.82            1.62
Si 14  K-series   7.27    7.36    6.69            0.37
Ti 22  K-series   1.98    2.01    1.07            0.16
Zr 40  L-series   0.48    0.49    0.14            0.08
C   6  K-series   0.00    0.00    0.00            0.00
------------------------------------------------------
         Total:  98.80  100.00  100.00
```

Figure 1: SEM and EDX of a FMAL, mean size 20nm, BET 199 m^2/g

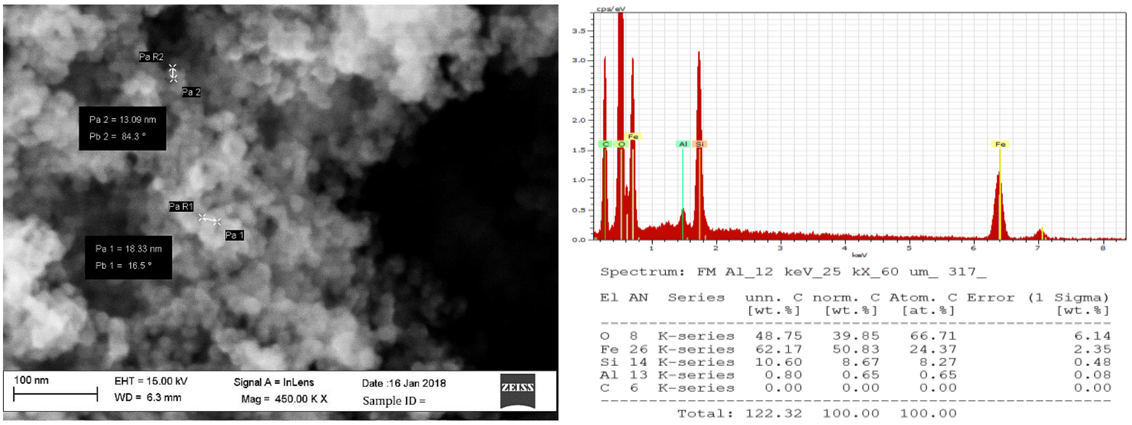

```
Spectrum: FM Al_12 keV_25 kX_60 um_ 317_

El AN  Series   unn. C norm. C Atom. C Error (1 Sigma)
                [wt.%]  [wt.%]  [at.%]          [wt.%]
------------------------------------------------------
O   8  K-series  48.75   39.85   66.71            6.14
Fe 26  K-series  62.17   50.83   24.37            2.35
Si 14  K-series  10.60    8.67    8.27            0.48
Al 13  K-series   0.80    0.65    0.65            0.08
C   6  K-series   0.00    0.00    0.00            0.00
------------------------------------------------------
         Total: 122.32  100.00  100.00
```

Figure 2: SEM and EDX of a FMZR sample, mean size 15nm, high purity (>99.9 %), BET 79 m^2/g

The materials are therefore similar in size, of high purity and exhibits interesting BET values. In detail, the average FMAL particle size was about 17-22 nm, whereas the FMZR particles were characterized by a slightly lower dimension, about 13-18 nm. Regarding the BET surface results, the FMAL particles showed a larger specific surface area, about 200 m^2/g, being more than 2-fold higher in comparison with that of FMZR (about 80 m^2/g).

3.2 As and MB removal tests

The efficiency of the materials was analysed following the procedure described in section 2.6, by using three different solutions: one with MB only, one with As only and the last one with MB and As mixed together.
Figure 3 and 4 displays the MB and As removal results.

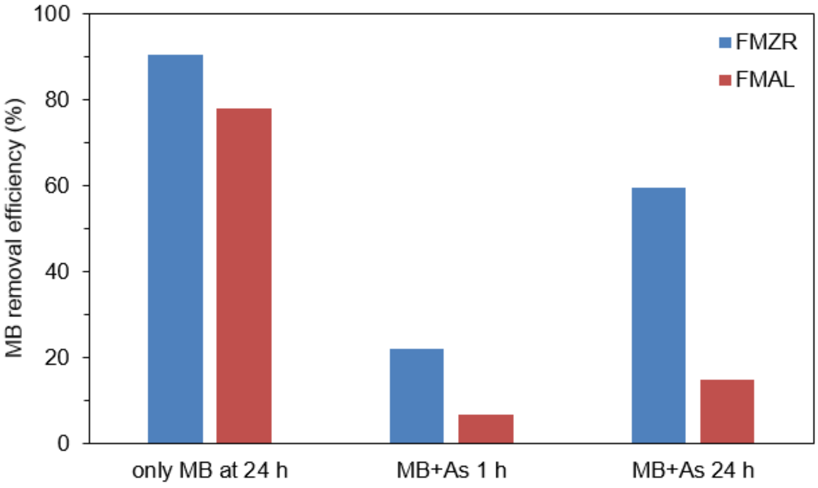

Figure 3: MB removal results using the two nano-materials in photocatalytic tests

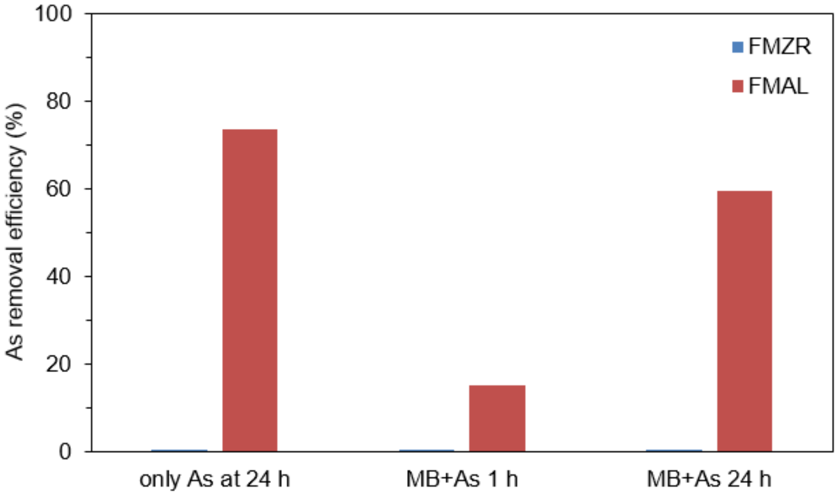

Figure 4: As removal results using the two nano-materials in adsorption tests

FMAL nanoparticles showed the highest As removal efficiency, reaching a value of 73.5 % when only As species were present in solution, and achieving a removal efficiency of about 59.5 % in the bi-component solution. Indeed, the FMZR nanoparticles did not show appreciable As removal efficiency. This was probably due to its superficial characteristics that were not suitable for the adsorption of As species in aqueous solutions, independently from the presence of other compounds. Another explanation could be that the FMZR particles at the solution pH (equal to 6) has a negatively surface charge, that cannot attract the As species, usually present in the oxyanion forms (AsO_3^{3-}). The FMAL nanoparticles showed also a remarkable MB removal efficiency, equal about to 78 % when only MB was present in solution; similar degradation efficiencies were reported in other studies (Houas et al., 2001). This value dropped significantly in the bi-component solution (the MB removal efficiency was about 15 %), probably due to the higher affinity of FMAL surface towards As, in comparison with MB. However, the highest MB removal efficiency was observed for FMZR that showed a noticeable photocatalytic removal efficiency of MB, equal about to 90.5 %. The obtained efficiencies were relatively high and thus satisfactory. On the contrary, adopting the mixed solution, the removal efficiencies of both materials sensibly reduced. The interference among MB and As was larger in the case of FMAL nano-materials, considering the MB photodegradation tests (the removal efficiency decreased from 78 % to 15 %) whereas the antagonistic influence of the two species was less remarkable in the As adsorption tests, for the same material. In order to remove both contaminants (organic matter and heavy metals), the best choice could be to use both materials in the same mixture solution, even if the FMAL particles application demonstrated more advantages with respect to FMZR ones, since this nano-particles can be successfully employed in both photocatalytics and adsorption tests. The two nanoparticles were both recovered after the 24 h photo-catalytic and adsorption tests, and only about 0.9 % of the powder remain in solution. In fact, the recovered nano-material mass was about 218 mg, in both cases.

4. Conclusions

The use of photocatalysis for the removal of emerging organic matter and the use of adsorption for the removal of heavy metal from contaminated water and wastewaters will be of increasing interest in the next future for safe water preparation purposes. Based on the obtained results during this work, it appears that the employed nanomaterials FMAL and FMZR nanoparticles are capable to remove 90.5 % of the organic matter (MB) and 73.5 % of heavy metals (As). Finally, the nanomaterial can be easily recovered from the water by magnets at 99.1 % of its initial mass. However, the FMAL catalyst demonstrated to be more suitable and versatile towards both MB and As removal, through photo-degradation or pure adsorption mechanism, in comparison with the FMZR particles. Even the here proposed technique may not solve completely the total decontamination of water streams of emerging pollutants nowadays, research should pursuit better efficiencies in the next future.

Acknowledgment

Financial support given by the GALILEO programme (G16-47) for staff exchange purposes is here gratefully acknowledged.

References

Bavasso I., Vilardi G., Stoller M., Chianese A., Di Palma L., 2016, Perspectives in nanotechnology based innovative applications for the environment, Chem. Eng. Trans., 47, 55-60.

Cheng K., Chhor K., Kanaev A., 2017, Elaboration and enhanced activity of the mixed oxide Zrx/Ti1-x/O2/nano-photocatalyst, Chem. Eng. Trans., 60, 37-42.

Chiavola A., D ’amato E., Stoller M., Chianese A., Boni M.R., 2016, Application of Iron Based Nanoparticles as Adsorbents for Arsenic Removal from Water. Chem. Eng. Trans., 47, 325–330.

Chinh V.D., Broggi A., Di Palma L., Scarsella M., Speranza G., Vilardi G., Thang P.N., 2018, XPS Spectra Analysis of Ti2+, Ti3+ Ions and Dye Photodegradation Evaluation of Titania-Silica Mixed Oxide Nanoparticles. J. Electron. Mater., 47, 2215–2224.

Crespi J., Quici N., Halac E. B., Leyva A. G., Ramosb C. P., Mizrahi M.,Requejo F., G., Litter M. I., 2016, Removal of uranium (VI) with iron nanoparticles, Chem. Eng. Trans., 47, 265-270.

Di Palma L., Medici F., Vilardi G., 2015, Artificial Aggregate From non Metallic Automotive Shredder Residue. Chem. Eng. Trans., 43, 1723-1728.

Gueye M.T., Di Palma L., Allahverdiyeva G., Bavasso I., Petrucci E., Stoller M., Vilardi G., 2016, The influence of heavy metals and organic matter on hexavalent chromium reduction by nano zero valent iron in soil, Chem. Eng. Trans., 47, 289-294.

Houas A., Lachheb H., Ksibi M., Elaloui E., Guillard C., Herrmann J.M., 2001, Photocatalytic degradation pathway of methylene blue in water, Appl. Catal. B Environ., 31, 145–157.

Marsili E., Beyenal H., Di Palma L., Merli C., Dohnalkova A., Amonette J. E., Lewandowski Z., 2005, Uranium removal by sulfate reducing biofilms in the presence of carbonates, Water Sci. Tech., 52, 49-55.

Marsili E., Beyenal H., Di Palma L., Merli C., Dohnalkova A., Amonette J. E., Lewandowski Z., 2007, Uranium immobilization by sulfate-reducing biofilms grown on hematite, dolomite, and calcite, Env. Sci. Tech., 41, 8349-8354.

Muradova G.G., Gadjieva S.R., Di Palma L., Vilardi G., 2016, Nitrates Removal by Bimetallic Nanoparticles in Water, Chem. Eng. Trans., 47, 205–210.

Rashid J., Barakat M.A., Ruzmanova Y., Chianese A., 2015, Fe3O4/SiO2/TiO2 nanoparticles for photocatalytic degradation of 2-chlorophenol in simulated wastewater, Environ. Sci. Pollut. Res., 22, 3149–3157.

Ruzmanova Y., Stoller M., Bravi M., Chianese A., 2015, A Novel Approach for the Production of Nitrogen Doped TiO 2 Nanoparticles, Chem. Eng. Trans., 43, 721–726.

Ruzmanova Y., Stoller M., Chianese A., 2013, Photocatalytic treatment of olive mill waste water by magnetic core titanium dioxide nanoparticles, Chem. Eng. Trans., 32, 2269–2274.

Stoller M., Azizova G., Mammadova A., Vilardi G., Di Palma L., Chianese A., 2016, Treatment of Olive Oil Processing Wastewater by Ultrafiltration, Nanofiltration, Reverse Osmosis and Biofiltration, Chem. Eng.

Trans., 47, 409–414.

Stoller M., Movassaghi K., Chianese A., 2011, Photocatalytic Degradation of Orange II in Aqueous Solutions by Immobilized Nanostructured Titanium Dioxide, Chem. Eng. Trans., 24, 229–234.

Stoller M., Ochando-Pulido J.M., Vilardi G., Vuppala S., Bravi M., Verdone N., Di Palma L., 2017a, Technical and economic impact of photocatalysis as a pretreatment process step in olive mill wastewater treatment by membranes, Chem. Eng. Trans., 57, 1171-1176.

Stoller M., Ochando-Pulido J.M., Di Palma L., Ferez A.M., 2015, Membrane process enhancement of 2-phase and 3-phase olive mill wastewater treatment plants by photocatalysis with magnetic-core titanium dioxide nanoparticles, J. Ind. Eng. Chem., 30, 147–152.

Stoller M., Vuppala S., Matarangolo M., Vaiano V., Sannino D., Chianese A., Cianfrini C., 2017b, About a novel production method for N-doped magnetic nanocore nanoparticles of titania by means of a spinning disk reactor, Chem. Eng. Trans., 60, 43-48.

Vaiano V., Sacco O., Sannino D., Stoller M., Ciambelli P. Chianese A., 2016, Photocatalytic removal of phenol by ferromagnetic N-TiO2/SiO2/Fe3O4 nanoparticles in presence of visible light irradiation, Chem. Eng. Trans., 47, 235-240.

Vilardi G., Di Palma L., 2017, Kinetic Study of Nitrate Removal from Aqueous Solutions Using Copper-Coated Iron Nanoparticles, Bull. Environ. Contam. Toxicol., 98, 359–365.

Vilardi G., Di Palma L., Verdone N., 2017a, Competitive Reaction Modelling in Aqueous Systems: the Case of Contemporary Reduction of Dichromates and Nitrates by nZVI, Chem. Eng. Trans., 60, 175–180.

Vilardi G., Stoller M., Verdone N., Di Palma L., 2017b, Production of nano Zero Valent Iron particles by means of a spinning disk reactor. Chem. Eng. Trans. 57, 751–756.

Vilardi G., Verdone N., Di Palma L., 2017c,. The influence of nitrate on the reduction of hexavalent chromium by zero-valent iron nanoparticles in polluted wastewater, Desalin. Water Treat., 86, 252–258.

Vilardi G., 2018, Bimetallic nZVI-induced chemical denitrification modelling using the shrinking core model. Chem. Eng. Trans., 70, 235-240.

Vilardi G., Di Palma L., Verdone N., 2018a, Heavy metals adsorption by banana peels micro-powder. Equilibrium modeling by non-linear models, Chinese J. Chem. Eng., 26, 455–464.

Vilardi G., Di Palma L., Verdone N., 2018b, On the critical use of zero valent iron nanoparticles and Fenton processes for the treatment of tannery wastewater, J. Water Process Eng., 22C, 109–122.

Vilardi G., Mpouras T., Dermatas D., Verdone N., Polydera A., Di Palma L., 2018c, Nanomaterials application for heavy metals recovery from polluted water: the combination of nano zero-valent iron and carbon nanotubes. Competitive adsorption non-linear modeling, Chemosphere, 201, 716-729.

Vilardi G., Ochando Pulido J.M., Verdone N., Stoller M., Di Palma L., 2018d, On the removal of Hexavalent Chromium by olive stones coated by iron-based nanoparticles: equilibrium study and Chromium recovery, J. Clean. Prod., DOI: 10.1016/j.jclepro.2018.04.151.

Vilardi G., Rodriguez-Rodriguez J., Ochando Pulido J.M., Verdone N., Di Palma L., 2018e, Pilot-Scale application of a real Tannery wastewater treatment by Fenton oxidation: Fe(II) and nZVI catalyst comparison and kinetic modelling, Process Saf. Environ. Prot., In press.

Vilardi G., Sebastiani D., Miliziano S., Verdone N., Di Palma L., 2018f,. Heterogeneous nZVI-induced Fenton oxidation process to enhance biodegradability of excavation by-products, Chem. Eng. J., 335, 309–320.